River Flow 2010 - Dittrich, Koll, Aberle & Geisenhainer (eds) - © 2010 Bundesanstalt für Wasserbau ISBN 978-3-939230-00-7

Spatial Variability in Turbulent Flows over Water-worked Gravel Beds

J. R. Cooper & S. J. Tait
School of Engineering, Design & Technology, University of Bradford, Bradford, UK

ABSTRACT: This paper describes a series of laboratory tests in which flow velocities have been measured in a detailed spatial pattern over a water-worked gravel bed. These data have been utilized to examine the level of flow spatial variability and its influence on momentum transfer. The results revealed significant degrees of spatial variation in time-averaged velocities, of a level to the temporal variability in instantaneous velocities. Spatial variability in turbulent intensities was substantially less than in time-averaged velocities. Form-induced stress was only significant within the roughness elements, and made contributions of up to 35 % to the fluid stress at the roughness crest. The results also indicated that there was significant spatial heterogeneity in Reynolds and form-induced momentum flux, and therefore in the manner in which momentum is transferred. The vertical variation in the level of flow spatial variability and form-induced stress was well scaled by bed geometry. In contrast at a given height above the bed, the relative magnitude of the spatial variability and form-induced stress was greater with a reduction in relative submergence. It implied that the spatial coherency in the flow is well controlled by bed geometry, and the level of spatial heterogeneity at a given height is also dependent on relative submergence.

Keywords: Turbulent flow, Channel flow, River beds, Spatial analysis, flow patterns

1 INTRODUCTION

The surface of a water-worked gravel bed displays a spatially complex, three-dimensional, structure. Any study of the interaction between the fluid and the bed must be able to examine the relationship between this structure and the spatial characteristics of the turbulent flow. It is well established that turbulent flows exhibit coherence in both time and space. For example, several studies have reported on the existence of vortically-based, depth-scale flow structures over water-worked gravel surfaces. It has been shown that flow depth has an important control on the size of these large-scale flow structures. The structures are typically of a scale of 3 to 5 flow depths in length and their lateral and vertical extent is more or less equal to one flow depth (Shvidchenko & Pender, 2001; Roy et al., 2004). This scaling with flow depth has also been revealed in the level of spatial variability in the turbulent properties of the flow. It has been reported that this level increases with a rise in relative submergence (Lamarre & Roy, 2005; Buffin-Bélanger et al., 2006).

It is also known that the time-averaged flow over water-worked gravel beds is spatially heterogeneous and three-dimensional, and is strongly controlled by relative submergence (Lamarre & Roy, 2005; Legleiter et al., 2007; Aberle et al., 2008, Cooper & Tait, 2008; Hardy et al., 2009). For example, it has been reported that the level of spatial variability in the time-averaged velocity also increases with a rise in relative submergence (Clifford, 1996; Buffin-Bélanger et al., 2006). At the reach scale, Legleiter et al., (2007) concluded that an increase in flow stage results in the spatial structure of time-averaged velocity becoming smoother and more continuous. They also reported a stage-dependent effect of local boundary roughness on the time-averaged flow. The reach-scale flow pattern was found to primarily reflect the bulk morphology of the channel, but the more localized influence of bed surface topography was increasingly smoothed out as flow depth increased. Lamarre & Roy (2005) also concluded that the distribution of the mean flow properties displayed a well organized, coherent spatial pattern that was controlled by flow depth rather than

by abrupt, isolated changes associated with individual clasts. This had led to the conclusion that flow depth is the primary control on flow structure in gravel-bed rivers (Roy et al., 2004; Lamarre & Roy, 2005; Legleiter et al., 2007).

Nikora et al. (2001) proposed a theoretical framework which could be used to account explicitly for the effects of this spatial coherency on the momentum exchange between a porous bed and a turbulent flow. It stated that time-averaging of the Navier-Stokes equation should be supplemented with spatial area averaging in the plane parallel to the averaged bed surface. When combined with a spatial decomposition of velocity, this produces a new term in the momentum balance equation, form-induced stress, which accounts for the contribution of the spatial heterogeneity in time-averaged flow to momentum transfer. Aberle et al. (2007; 2008) showed that the form-induced stress within the roughness elements can account for up to 40 to 50 % of the shear stress experienced at the roughness crest, and that the shape of the profiles was strongly influenced by roughness geometry. Their results also showed that, in relative terms, form-induced stress contributes more significantly to the momentum budget in shallow flows than flows with a high submergence.

These studies reveal that relative submergence has an important control on the spatial properties of flows over water-worked gravel beds, but no study has attempted to quantify the level of spatial variability in both the turbulent and time-averaged flow properties, and how this relates to changes in submergence. This paper describes a series of tests in which flow velocities have been measured in a detailed spatial pattern over a water-worked gravel bed. The data has been used to study the spatial flow characteristics for a range of flow submergences. The aim of the paper is to (1) quantify the level of spatial variability and how this influences momentum transfer between the flow and the bed, and (2) to describe how this changes with relative submergence.

2 METHODOLOGY

The tests were conducted in a tilting, 18.3 m long, 0.5 m wide laboratory flume. A sediment deposit was formed by feeding in a mixture with a slightly bimodal grain-size distribution into running water, with the feed rate being twice the estimated transport capacity of the flow. The mixture was composed of 75 % gravel and 25 % sand, had a median grain diameter D_{50} of 4.41 mm and a range $0.15 < D < 14$ mm. The surface was water-worked and armored, but contained no significant bedforms. Six tests were carried out at different relative submergences at a single bed slope (Table 1). The selected flow conditions were below those required for bed movement, so the bed surface topography did not change during each test. The flows were steady, uniform and fully turbulent.

A 2-D Particle Image Velocimetry (PIV) system was used to provide detailed spatial measurements of fluid velocity over the bed. It was operated at 9 Hz, and the flow was sampled for five and a half minutes. PIV measurements were taken in a vertical plane at nine lateral positions across the bed: -88 mm, -66 mm, -44 mm, -22 mm, 0 mm, 22 mm, 44 mm, 66 mm, 88 mm. A lateral position of 0 mm denotes the centreline of the flume. At each lateral position a streamwise length of 144 mm was imaged and the measurement area was 9.1 m from the flume inlet. This configuration enabled streamwise and vertical velocities to be measured both within the roughness elements and up to the water surface, at different streamwise and vertical positions. A maximum of 61 velocity measurements was provided in the streamwise direction at each lateral position. The maximum number of measurements available for spatial averaging was therefore 549 at a given measurement height. The separation distance between measurements, in both the streamwise and vertical direction, was 2.25 mm.

For each experimental run, the instantaneous velocities u were used to derive turbulence and spatial flow characteristics. This was achieved by time averaging these velocities and applying a Reynolds decomposition. This was supplemented with spatial averaging and a spatial decomposition, see Nikora et al. (2001). The averaging procedure for spatial area averaging at level z is defined according to Nikora et al. (2001) in Eq. (1) as

$$\langle V \rangle(x,y,z,t) = \frac{1}{A_f} \int_{A_f} \int V(x,y,z,t) dx dy \qquad (1)$$

where V is the flow velocity defined in the fluid to be spatially-averaged over the fluid domain A_f. The displacement z is defined as the vertical distance from the minimum bed surface elevation. The averaging domain is assumed to be planar and parallel to the bed surface. The averaging area A_f is taken to be a thin, planar slab in order to preserve the characteristic spatial variability in the flow in the vertical direction. Eq. (1) was combined with a decomposition of time-averaged variables into spatially averaged and spatially fluctuating components, such that $\overline{u} = \langle \overline{u} \rangle + \widetilde{u}$. The spatial fluctuations arise from the difference between the double-averaged $\langle \overline{u} \rangle$ and time-averaged $\overline{u}$ values, similar to the conventional

Reynolds decomposition of $u' = u - \overline{u}$. The analysis will concentrate on the spatial properties of the near-bed flow by examining the form-induced intensities $\sqrt{\langle \widetilde{u}^2 \rangle}$ and $\sqrt{\langle \widetilde{w}^2 \rangle}$, form-induced stress $\langle \widetilde{u}\widetilde{w} \rangle$ and the spatial variability in turbulence intensities $\sqrt{\overline{u'^2}}$ and $\sqrt{\overline{w'^2}}$, and in Reynolds stress $\overline{u'w'}$.

In this paper the shear velocity is defined by $u_* = \sqrt{\tau_0 / \rho}$ where τ_0 is the total fluid stress at the roughness crest (maximum bed elevation), as suggested by Manes et al. (2007). The total fluid stress was estimated by extrapolating the spatially-averaged Reynolds stress from the flow layer above the bed surface down to the roughness crest. Manes et al. (2007) argue that the shear velocity at the roughness crest rather than the roughness trough is the most appropriate scaling parameter when dealing with flows with a range of relative submergences. The relative height above the minimum bed elevation is defined as z/k, where k is the bed geometric roughness height approximated by the range of bed surface elevations.

Table 1. A summary of the experimental conditions, where S is the bed slope, Q is the flow discharge, d is the flow depth, k is the bed geometric roughness height.

Test	S (-)	Q (m^3/s)	d (m)	d/k (-)
1	0.00284	0.00143	0.0173	1.3
2	0.00284	0.00276	0.0272	2.0
3	0.00284	0.00527	0.0373	2.7
4	0.00284	0.00809	0.0455	3.3
5	0.00284	0.0127	0.0595	4.3
6	0.00284	0.0245	0.0845	6.2

3 RESULTS AND DISCUSSION

3.1 *Form-induced intensities*

The vertical profiles of the relative streamwise form-induced intensity $\sqrt{\langle \widetilde{u}^2 \rangle}/u_*$ are shown in Figure 1a. This intensity is simply the standard deviation in $\overline{u}$ over the bed scaled by u_* and is a measure of the relative degree of spatial variability in $\overline{u}$. The profiles for the six tests demonstrate that the values of $\sqrt{\langle \widetilde{u}^2 \rangle}/u_*$ differ greatly but they all exhibit the same general form. The level of spatial variability is low close to the water surface and then it increases towards the bed surface until it attains its maximum value within the roughness elements. From this height $\sqrt{\langle \widetilde{u}^2 \rangle}/u_*$ quickly reduces towards the roughness trough. The consistency in the profile shape within the roughness elements reveals the strong control of bed geometry on the vertical variation in $\sqrt{\langle \widetilde{u}^2 \rangle}/u_*$. Another control is also apparent. At similar measurement heights $\sqrt{\langle \widetilde{u}^2 \rangle}/u_*$ tends to be higher at the lower submergences, and this even occurs within the roughness elements.

Of particular interest is that $\sqrt{\langle \widetilde{u}^2 \rangle}/u_*$ is not negligible above the bed surface, in the region where the flow has often been assumed to not be influ enced by individual roughness elements. It has been argued that the upper boundary of the form-induced layer may be defined as the position where $\sqrt{\langle \widetilde{u}^2 \rangle}/u_*$ reduces to some low, threshold level, because $\sqrt{\langle \widetilde{u}^2 \rangle}/u_*$ indicates where there is significant spatial variability in $\overline{u}$ and therefore determines the conditions for the development of the logarithmic layer (Pokrajac et al., 2007). Alternatively it as the level at which there is a significant increase in $\sqrt{\langle \widetilde{u}^2 \rangle}/u_*$ towards the bed surface or the height at which $\sqrt{\langle \widetilde{u}^2 \rangle}/u_*$ becomes fairly invariant with height. The profile shape is reasonably consistent for the different submergences, but it is not possible to unambiguously define the upper boundary of the form-induced layer using any of these criteria. This will be explored further in respect of profiles of form-induced stress below.

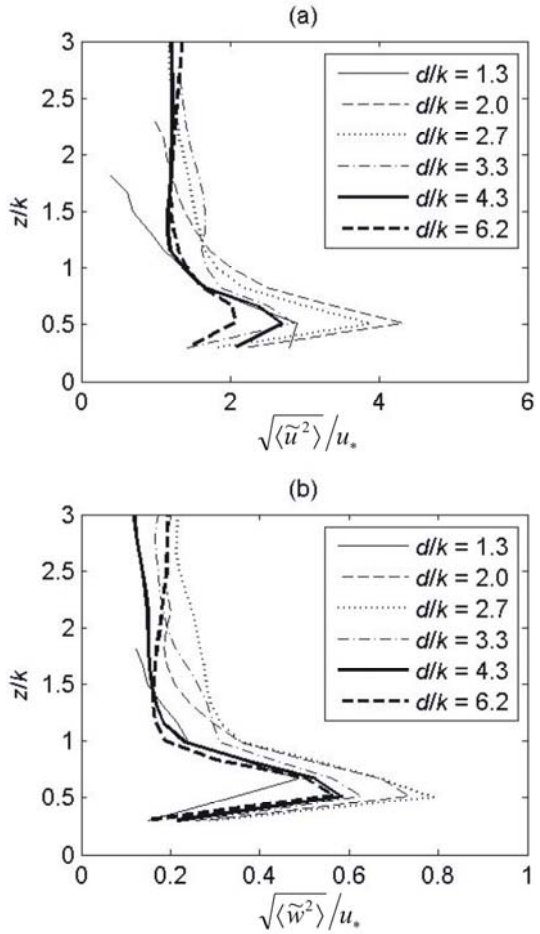

Figure 1. Vertical profiles of (a) streamwise form-induced intensity and (b) vertical form-induced intensity. Note the different scales on the horizontal axes.

The shape of the profiles in Figure 1a, particularly those at the mid to lower relative submergences, compare favorably with those found by Aberle et al. (2007; 2008), particularly in regard to the level of spatial variability not always decreasing to a

negligible value within the flow layer above the bed. Aberle et al. (2007; 2008) presented dimensional values of $\sqrt{\langle \tilde{u}^2 \rangle}$. If u_* is estimated from the depth-slope it shows that within the roughness layer the values of $\sqrt{\langle \tilde{u}^2 \rangle}/u_*$ in Aberle et al. (2007; 2008), at similar heights and levels of relative submergence, are of a similar magnitude to the values in Figure 1a. Above the bed surface, however, Aberle et al. (2007; 2008) typically found that $\sqrt{\langle \tilde{u}^2 \rangle}/u_*$ varied from 0.4 to 0.8, which is lower than which is observed in Figure 1a. Their data also shows that $\sqrt{\langle \tilde{u}^2 \rangle}/u_*$ increases with a rise in relative submergence, further confirming the important influence of flow depth on the level of spatial variability in $\overline{u}$. Buffin-Bélanger et al. (2006) do not present form-induced intensity values but instead examine the spread in the box plots of $\overline{u}$. They showed that this dimensional spread increases with a deepening of the flow but it is difficult to assess how this relationship would change relative to u_*.

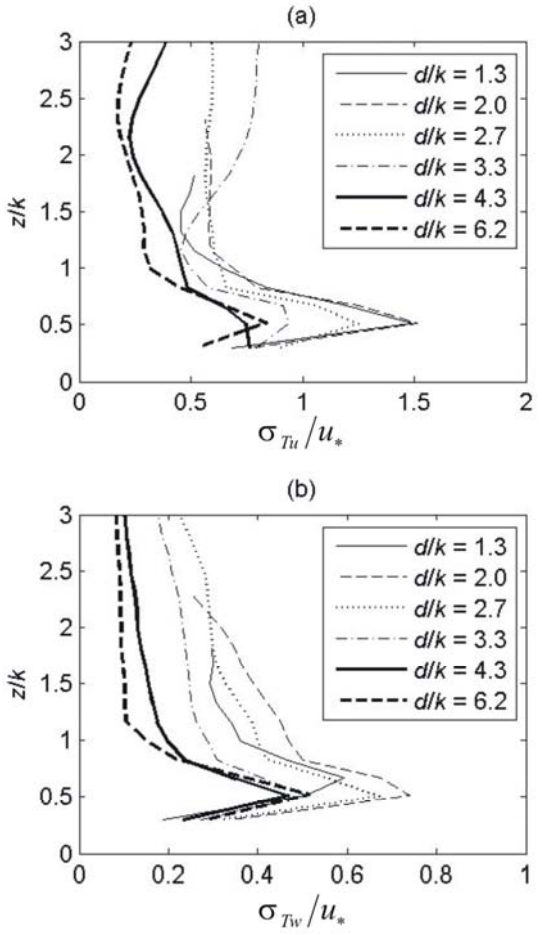

Figure 2. Vertical profiles of the standard deviations in (a) streamwise turbulence intensity and (b) vertical turbulence intensity. Note the different scales on the horizontal axes.

The level of spatial variability in $\overline{u}$ is similar to the level of temporal variability in u (given by turbulence intensity and not shown here). This demonstrates that the normal fluid stress is produced by stress caused by both turbulent and spatial fluctuations in the flow in near equal proportions. This has also been found by Coceal et al. (2007) in a direct numerical simulation of turbulent flows over staggered and square arrays of cubes.

Figure 1b displays the vertical profiles of the relative vertical form-induced intensity $\sqrt{\langle \tilde{w}^2 \rangle}/u_*$. It shows that the level of spatial variability in $\overline{w}$ is around a magnitude lower than it is for $\overline{u}$, which is less than half of the level of temporal variability in w. This suggests that the overall level of spatial variability in the time-averaged flow field is dominated by spatial variations in $\overline{u}$. The profile shape is very similar to that seen for $\sqrt{\langle \tilde{u}^2 \rangle}/u_*$, and displays the same dependency on relative submergence. No other study over gravel beds has quantified the level of spatial variability in $\overline{w}$. As far as we are aware only two other studies have examined values of $\sqrt{\langle \tilde{w}^2 \rangle}/u_*$ and these have both been for turbulent flows over spherical elements in laboratory flumes. Manes et al. (2007) examined how $\sqrt{\langle \tilde{w}^2 \rangle}/u_*$ varied with height and relative submergence over a uniform layer of glass balls. This was performed for relative submergences of 2.3 and 4. Within the roughness elements they discovered values of between 0.1 and 0.25, which is around a third to a half of the level of spatial variability seen in Figure 1b. Nikora et al. (2001) also examined the vertical profiles of $\sqrt{\langle \tilde{w}^2 \rangle}/u_*$ over spherical elements but at much higher relative submergences of 6.4 and 8.7. Their values are typically half of those in Figure 1b. This could be accounted for by the difference in bed geometry between a uniform arrangement of spherical elements and a spatially complex, 3D arrangement of grains on a water-worked gravel surface. Within the roughness elements the shape of the vertical profiles in both Manes et al. (2007) and Nikora et al. (2001) is similar to those in Figure 1b but above the bed surface their values only range from near-negligible to 0.1, much lower than over the water-worked gravel bed.

3.2 *Turbulence intensities*

The relative level of spatial variability in streamwise turbulence intensity is given by the standard deviation in turbulence intensity over the bed, symbolized by σ_{Tu}/u_*. The profiles in Figure 2a reveal that the level of spatial variability in streamwise turbulence intensity is typically half of the level of spatial variability in $\overline{u}$. There is a consistent tendency for σ_{Tu}/u_* to decrease with a rise in relative submergence, as has been seen previously. This is particularly pronounced within the roughness elements. We are not aware of any other study which has quantified the level of spatial variability in turbulence intensity.

Similar results can also be seen for the relative level of spatial variability in vertical turbulence intensity σ_{Tw}/u_* (Figure 2b). These values are smaller than for σ_{Tu}/u_*, suggesting that the overall level of spatial variability in the turbulence intensity flow field is largely dominated by spatial variance in $\sqrt{\overline{u}'^2}$. The values of σ_{Tw}/u_* are similar in magnitude to those for the vertical form-induced intensity. This shows that the level of spatial variability in the vertical velocity component is well matched in the turbulent and time-averaged flow parameters.

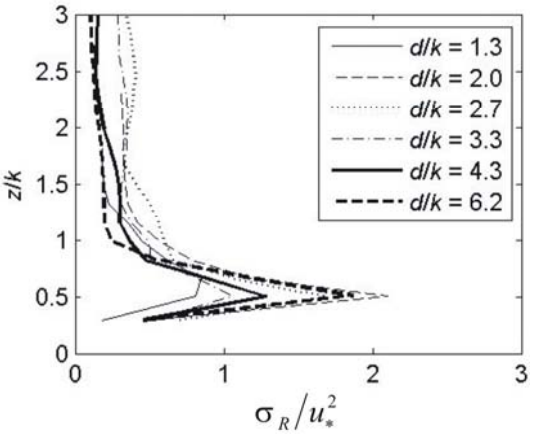

Figure 3. Vertical profiles of the standard deviation in Reynolds stress.

3.3 *Reynolds stress*

The relative level of spatial variability in Reynolds stress σ_R/u_*^2 (standard deviation in space) also displays a similar profile shape (Figure 3). This reveals that spatial heterogeneity in Reynolds stress is also closely related to bed geometry. The level of spatial variation in Reynolds stress in the flow above the bed is around 10 to 50 % of the stress at the roughness crest, and up to nearly three times higher within the roughness elements. Within this flow layer the spatially-averaged Reynolds stress reduces with height and the values of σ_R/u_*^2 are higher, so the spatial variability in Reynolds stress becomes more pronounced relative to its spatial mean. This suggests that an accurate estimation of spatially-averaged Reynolds stress becomes difficult within the roughness elements. A consistent influence of relative submergence on the values of σ_R/u_*^2 is only apparent above the bed surface.

Coceal et al. (2007) discovered similar profile shapes for σ_R/u_*^2 but much lower values. Within the roughness elements their values ranged from 0.05 to 0.4, and up to 0.04 above the arrays. This is substantially lower than is observed in Figure 3 and is possibly accounted for by the different geometrical arrangement of the individual roughness elements.

3.4 *Form-induced stress*

The vertical profiles of relative form-induced stress $-\langle\widetilde{u}\widetilde{w}\rangle/u_*^2$ are shown in Figure 4a. This term arises from the correlations between point-to-point spatial deviations in time-averaged velocity. It therefore depends on both the spatial coherence and level of spatial variability in the time-averaged flow. The profiles show that for the flow region above the bed, form-induced stress has a negligible contribution to the shear stress experienced at the roughness crest. At a height, which corresponds well with the roughness crest, $-\langle\widetilde{u}\widetilde{w}\rangle/u_*^2$ begins to become more significant, revealing the upper boundary of the flow layer (form-induced layer) which is influenced by the roughness beneath. The values of $-\langle\widetilde{u}\widetilde{w}\rangle/u_*^2$ then continue to increase reaching a first peak at a height which corresponds with the peaks in the levels of spatial variability observed above. Below this height $-\langle\widetilde{u}\widetilde{w}\rangle/u_*^2$ either reduces or switches from making a negative to a positive contribution to the total fluid stress. This switch in sign and existence of peaks within the roughness elements is due to the dependence of form-induced stress on the sign of $\widetilde{u}$ and $\widetilde{w}$, and hence on the manner in which the time-averaged flow is coherently structured. The shape of the profiles is consistent across the different levels of relative submergence. This reveals that roughness geometry has a strong control on the coherency of the flow within roughness elements, and that the flow is organized in a similar manner. This would suggest than an analysis of $-\langle\widetilde{u}\widetilde{w}\rangle/u_*^2$ can reveal the important effects of surface topography on flow structure.

At some positions within the roughness elements, form-induced stress can make a large contribution to the fluid stress at the roughness crest, typically up to 10-35 %. This reveals form-induced stress is a significant component in the momentum balance within the surface of water-worked gravel beds. This would indicate that an accurate estimate of the fluid stress within the roughness elements can be only be obtained by taking into account both the Reynolds and form-induced stress. Within the roughness elements $-\langle\widetilde{u}\widetilde{w}\rangle/u_*^2$ is typically higher at the lower submergences, which coincides well with the results presented for $\sqrt{\langle\widetilde{u}^2\rangle}/u_*$ and $\sqrt{\langle\widetilde{w}^2\rangle}/u_*$. Therefore the relative role of form-induced stress in transferring momentum is dependent on relative submergence within this flow region. The similarity in the profile shapes within the roughness elements suggests that this is predominantly driven by differences in the level of spatial variability in $\overline{u}$ and $\overline{w}$, and not differences in spatial coherency.

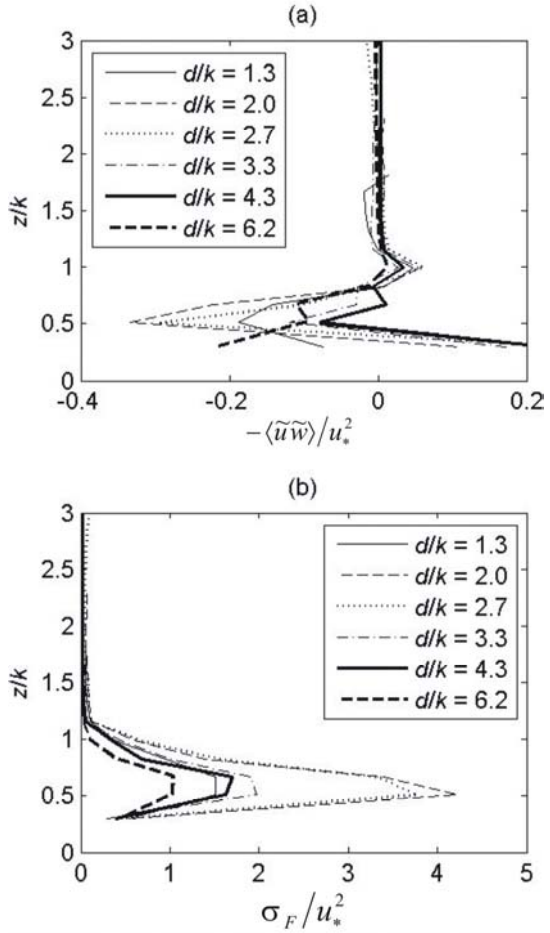

Figure 4. Vertical profiles of (a) form-induced stress and (b) standard deviation in form-induced momentum flux. Note the different scales on the horizontal axes.

The profiles of $-\langle\widetilde{u}\widetilde{w}\rangle/u_*^2$ in Figure 4a bear a close resemblance to those in Aberle et al. (2007; 2008) and they too concluded that the shape is a reflection of the geometry of the bed. Their results also reveal, when analyzed in relative terms, that form-induced stress contributes more significantly to the momentum budget in shallow flows than flows with a high submergence. This has also been reported by Manes et al. (2007) and theoretically confirmed using dimensional analysis arguments by Gimenez-Curto & Corniero Lera (1996).

The difference between the results in Figure 4a and those by Aberle et al. (2007; 2008), however, is in the level of contribution which form-induced stress makes within the roughness elements. Aberle et al. (2008) showed that $-\langle\widetilde{u}\widetilde{w}\rangle/u_*^2$ can obtain values of up to around 60 % (typically up to 40 to 50 %), higher than observed in Figure 4a. Aberle et al. (2008) conceded that the magnitude of form-induced stress cannot be unambiguously determined from point velocity measurements but that the number of measurement locations does not influence the shape of the profiles. Therefore, given the similarity in the shapes between those in Figure 4a and those in Aberle et al. (2007; 2008) it would appear sensible to conclude that the difference in magnitude could be linked to the difference in the number of measurement locations used to estimate $-\langle\widetilde{u}\widetilde{w}\rangle/u_*^2$.

The profiles of the relative level of spatial variability in form-induced momentum flux σ_F/u_*^2 display a similar shape to those seen earlier, except for the flow region above the roughness elements where σ_F/u_*^2 is negligible (Figure 4b). For the majority of experimental tests, the values of σ_F/u_*^2 within the roughness elements are similar to those for σ_R/u_*^2. The values of σ_F/u_*^2 and σ_R/u_*^2 indicate that there is significant spatial variability in the manner in which momentum is transferred over the bed. From Figure 4a it is known that form-induced stress is lower than Reynolds stress at a given height. This reveals that there is much greater spatial variation in form-induced momentum flux around its spatial mean than for Reynolds stress. Within the roughness elements, the standard deviation in form-induced momentum flux is typically a decade higher than the spatially-averaged form-induced stress. This indicates that form-induced flux is highly spatially variable. The values of σ_F/u_*^2 are higher at the lower submergences, indicating that it is most difficult to obtain a spatially representative estimation of form-induced stress for shallower flows.

To illustrate this further Figure 5 shows the probability density functions of $-\widetilde{u}\widetilde{w}/u_*^2$ taken from measurements at single locations over the bed. It displays the $-\widetilde{u}\widetilde{w}/u_*^2$ values (non-spatially-averaged) for each measurement location. To gain an understanding of the spatial scale each individual measurement represents, the separation distance between measurement locations and the height of the averaging slab was 2.265 mm, so the $\widetilde{u}\widetilde{w}$ values were taken from a measurement area of 5.130 mm^2 (the PIV interrogation area). Assuming that the area of the median grain on the bed can be approximated by the area of a circle, the median grain is 15.31 mm^2 in area. Comparing this area to the measurement area of 5.130 mm^2, it means that the form-induced fluxes are being examined at the sub-grain scale in Figure 5. This is carried out using measurements at the lowest measurement height within the roughness elements (z/k = 0.47) and at the roughness crest (z/k = 1.01).

Within the roughness elements, the distributions have a well defined peak and long tails (Figure 5a). The shape is similar for each of the flow conditions, further showing the consistent influence which the roughness geometry has on the spatial distribution and therefore the vertical profile of $-\langle\widetilde{u}\widetilde{w}\rangle/u_*^2$ within this flow layer. A similar distribution shape has also been found for the distributions of Reynolds stress fluctuations over time (e.g. Antonia & Atkinson, 1973; Nakagawa & Nezu, 1977). For Reynolds stress this would

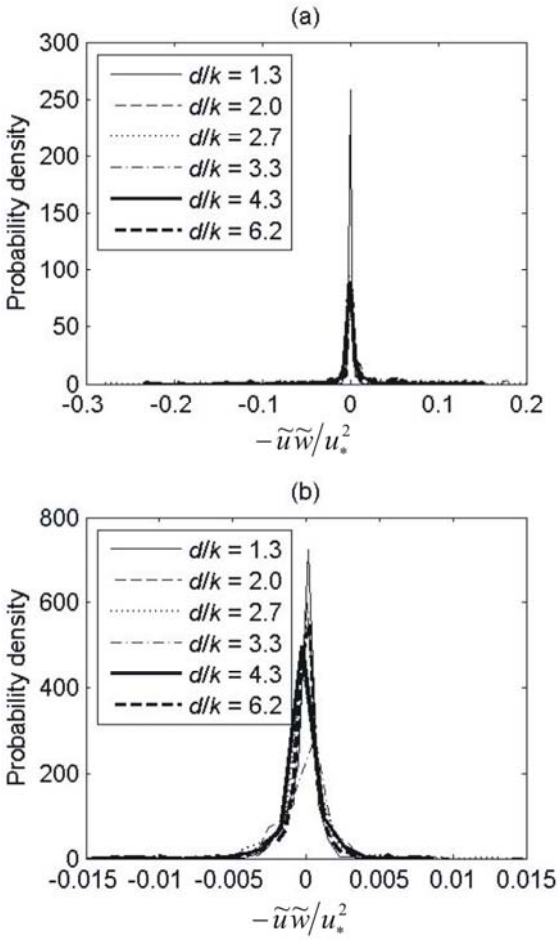

Figure 5. Probability density functions of form-induced momentum flux at single measurement locations at (a) z/k = 0.47 and (b) z/k = 1.01. Note the different scales on the horizontal and vertical axes.

indicate that Reynolds stress is predominately caused by a small number of highly correlated streamwise and vertical temporal fluctuations and/or highly turbulent events. Extending these thoughts to the spatial domain, the well defined peak and long tails reveal that form-induced stress is predominately created by highly correlated streamwise and vertical motions in a small number of areas of the bed and/or highly spatially variable flow.

At the lowest measurement location within the roughness elements, it can be seen that the long tails indicate that some locations over the bed can make both positive and negative contributions of up to 20 to 30 % to the fluid stress at the roughness crest. This is very similar to the results of Nikora et al. (2001) and supports the assertion of Manes et al. (2008) that form-induced stress is "noisy". The range of $-\widetilde{u}\widetilde{w}/u_*^2$ values is very large, around double the spatial mean. This is smaller than the range reported in Aberle et al. (2008), in which the range was more than a magnitude higher than the spatial mean. This is likely to be because their bed was composed of much larger roughness elements. The distributions in Figure 5a demonstrate that form-induced momentum flux over some areas of the bed is likely to contribute significantly to the fluid stress and the converse will happen over other areas of the bed. It means that variable estimates of form-induced stress can be obtained across the bed, depending on the number and location of velocity measurements, as was also shown in Aberle et al. (2008). Measurements over some areas of the bed are likely to over-predict heavily form-induced stress, whilst others will significantly under-predict form-induced stress. For example, form-induced flux contributions at some positions could be more than double that at other positions over the bed. This has important consequences when trying to accurately measure a spatially representative estimate, as discussed by Manes et al. (2008). This appears to not be so important at the roughness crest (Figure 5b) because the range of values is smaller, the distribution spreads more progressively and there are fewer instances of extreme, high values of $-\widetilde{u}\widetilde{w}/u_*^2$.

For each of the measures of flow spatial variability described above, it has been observed that the profile shape is similar for flows across a range of relative submergences, but that at the same measurement heights the relative magnitude of these parameters is dependent on submergence. It suggests that the spatial characteristics of the near-bed flow field are controlled by both bed geometry and relative submergence. The consistency in the profile shape suggests that the organisation of the flow and its spatial coherency is well controlled by the former, and the relative level of spatial heterogeneity at a given height is also dependent on the latter. This has been shown to occur for flows of mid to high relative submergences over a macroscopically flat, water-worked gravel bed which exhibits no significant bedforms. Future work will examine whether this is the case for beds with isolated roughness elements and bedforms, where the control of bed geometry might be assumed to be stronger. No examination has been made of the spatial structure of turbulent flow structures, but the results do support the conclusions of field-studies in which these bed features occurred, which showed that flow depth has an important control on the flow structure over water-worked gravel beds (Roy et al., 2004; Lamarre & Roy, 2005; Legleiter et al., 2007).

4 CONCLUSIONS

The paper describes a series of laboratory experiments in which flow velocities have been measured in detail over a water-worked gravel bed. These data have been utilized to examine the level of flow spatial variability and its influence on

momentum transfer. The results reveal significant degrees of spatial variation in time-averaged velocities, of a similar magnitude to the level of temporal variability in instantaneous velocities. Spatial heterogeneity in turbulence intensity was found to be half of the level found in the time-averaged flow parameters, and spatial variability in Reynolds stress was an order of a magnitude lower. This revealed that spatial variability in the turbulent parameters is substantially less than in time-averaged velocities.

The contribution of spatial heterogeneity in time-averaged flow to momentum transfer was characterized by estimating the form-induced stress. It was found to be only significant within the roughness elements, and made contributions of up to 35 % to the fluid stress experienced at the roughness crest. This indicated that, due to spatial coherency in the time-averaged flow field within this flow layer, measurements of Reynolds stress alone, whether spatially-averaged or not, cannot be used to determine shear stress.

The results indicated that there was significant spatial heterogeneity in Reynolds stress and form-induced momentum flux relative to their spatial means, and therefore also in the manner in which momentum is transferred over the bed. This has important consequences for producing spatially representative estimates of these two stress components within the roughness elements. The results showed that this is likely to be most difficult for shallow flows.

The vertical variation in the level of flow spatial variability and form-induced stress was well scaled by bed geometry. In contrast at a given height above the bed, the relative magnitude of the spatial flow variability and form-induced stress was greater with a reduction in relative submergence. It suggested that the relative roles of different momentum transfer mechanisms will change according to the depth of the flow. It implies that for water-worked gravel beds, where the roughness density is relatively high, the spatial coherency in the flow is well controlled by the bed geometry, and the level of spatial heterogeneity at a given height is also dependent on relative submergence.

REFERENCES

Aberle, J., Koll, K., and Dittrich, A. 2007. Analysis of form induced stresses over rough gravel-bed armour layers. Proceedings of XXXII IAHR Congress, Venice, CD-ROM.

Aberle, J., Koll, K., and Dittrich, A. 2008. Form induced stresses over rough gravel-beds. Acta Geophysica, 56(3), 584-600.

Antonia, R.A., and Atkinson, J.D. 1973. High-order moments of Reynolds shear-stress fluctuations in a turbulent boundary-layer. Journal of Fluid Mechanics, 58(8), 581-593.

Buffin-Bélanger, T., Rice, S., Reid, I., and Lancaster, J. 2006. Spatial heterogeneity of near-bed hydraulics above a patch of river gravel. Water Resources Research, 42; DOI:10.1029/2005WR004070.

Clifford, N.J. 1996. Morphology and stage-dependent flow structure in a gravel-bed river. Coherent Flow Structures in Open Channels. In Ashworth, PJ, Bennett, SJ, Best, JL, McLelland, SJ (eds). Chichester: John Wiley & Sons, 545-566.

Coceal, O., Thomas, T.G., and Belcher, S.E. 2007. Spatial variability of flow statistics within regular building arrays. Boundary-Layer Meteorology, 125(3), 537-552.

Cooper, J.R., and Tait, S.J. 2008. The spatial organisation of time-averaged streamwise velocity and its correlation with the surface topography of water-worked gravel beds. Acta Geophysica, 56(3), 614-641.

Gimenez-Curto, L.A., and Corniero Lera, M.A.C. 1996. Oscillating turbulent flow over very rough surfaces. Journal of Geophysical Research, 101(C9), 20745-20758.

Hardy, R.J., Best, J.L., Lane, S.N., and Carbonneau, P.E. 2009. Coherent flow structures in a depth-limited flow over a gravel surface: the role of near-bed turbulence and influence of Reynolds number. Journal of Geophysical Research, 114; DOI:10.1029/2007JF000970.

Lamarre, H., and Roy, A.G. 2005. Reach scale variability of turbulent flow characteristics in a gravel-bed river. Geomorphology, 68(1-2), 95-113.

Legleiter, C.J., Phelps, T.L., and Wohl, E.E. 2007. Geostatistical analysis of the effects of stage and roughness on reach-scale spatial patterns of velocity and turbulence intensity. Geomorphology, 83(3-4), 322-345.

Manes, C., Pokrajac, D., and McEwan, I. 2007. Double-averaged open-channel flows with small relative submergence. Journal of Hydraulic Engineering, ASCE, 133(8), 896-904.

Manes, C., Pokrajac, D., Coceal, O., and McEwan, I. 2008. On the significance of form-induced stress in rough wall turbulent boundary layers. Acta Geophysica, 56(3), 845-861.

Nakagawa, H., and Nezu, I. 1977. Prediction of contributions to Reynolds stress from bursting events in open-channel flows. Journal of Fluid Mechanics, 80(4), 99-128.

Nikora, V., Goring, D., McEwan, I., and Griffiths, G. 2001. Spatially averaged open-channel flow over rough bed. Journal of Hydraulic Engineering, ASCE, 127(2), 123-133.

Pokrajac, D., Campbell, L.J., Nikora, V., Manes, C., and McEwan, I. 2007. Quadrant analysis of persistent spatial velocity perturbations over square-bar roughness. Experiments in Fluids, 42(3), 413-423.

Roy, A.G., Buffin-Belanger, T., Lamarre, H., and Kirkbride, A.D. 2004. Size, shape and dynamics of large-scale turbulent flow structures in a gravel-bed river. Journal of Fluid Mechanics, 500, 1-27.

Shvidchenko, A.B., and Pender, G. 2001. Macroturbulent structure of open-channel flow over gravel beds. Water Resources Research, 37(3), 709-719.